https://doi.org/10.15407/ujpe71.2.100

I.P. IVANOV

School of Physics and Astronomy, Sun Yat-sen University
(Daxue rd. 2, Tangjiawan, Zhuhai, Guangdong, 519082, China; e-mail: ivanov@sysu.edu.cn)

VORTEX STATES AS A NOVEL TOOL FOR NUCLEAR AND PARTICLE PHYSICS [1]

Vortex states of photons, electrons, and other particles are wave packets with helical wave fronts, which carry an intrinsic orbital angular momentum (OAM) projection along their average propagation direction. Such states have already been produced experimentally, albeit at low energies, and there are prospects to extend them into the MeV and GeV energy ranges. The adjustable OAM carried by such wave packets represents a completely new degree of freedom never exploited in particle and nuclear collisions. Anticipating future experimental progress, one can ask what insights into nuclei and particles may be gained once collisions of high-energy vortex states become possible. Here, we discuss the present-day situation and outline the landscape of physics opportunities offered by high-energy vortex state collisions.

Keywords: vortex states, orbital angular momentum, proton spin puzzle.

1. Vortex States: A Brief Introduction

When describing high-energy collisions, one usually assumes the initial state particles to be well approximated by plane-wave. Real collisions take place between wave packets of finite extent; however, in nearly all realistic situations, this fact does not play any significant role and does not modify the differential cross sections or spin-dependent variables.

Recently, a new direction of research has emerged, in which one studies collisions of photons, electrons, and other particles prepared in the so-called vortex states, see [1–4] for recent reviews and [5] for an extension to other structured wave packets. A vortex state is described by a coordinate-space wave function $\psi(\mathbf{r})$ that, when written in cylindrical coordinates $(r_\perp, \varphi_r, z)$, depends on the azimuthal angle φ_r via the phase factor $\exp(i\ell\varphi_r)$, with an integer winding number ℓ. It is this factor that leads to a non-zero intrinsic OAM carried by this state (see Fig. 1). Note that this OAM is not a collective effect but a feature of each quantum of this state. Since the phase φ_r is undefined at $r_\perp = 0$, the wave function must vanish on the axis: $\psi(r_\perp = 0) = 0$. The resulting phase vortex line is topologically protected (cannot abruptly end), which renders vortex states remarkably stable during propagation from a source to the collision point.

Additional insights into the structure of a vortex state can be gained in momentum space. As is well known, a plane wave with momentum $\mathbf{k}_0$ is represented in momentum space by a delta function: $\phi(k) \propto \delta^{(3)}(\mathbf{k}-\mathbf{k}_0)$. In contrast, the momentum space wave function of the simplest vortex state, the so-called Bessel state, is

$$\phi(\mathbf{k}) \propto \delta(k_z - k_{0z})\,\delta(|k_\perp| - \varkappa)\,e^{i\ell\varphi_k}. \qquad (1)$$

In simple terms, a Bessel state is a superposition of plane waves with equal energy, longitudinal momentum, and the modulus of the transverse momentum

Citation: Ivanov I.P. Vortex states as a novel tool for nuclear and particle physics. *Ukr. J. Phys.* **71**, No. 2, 100 (2026). https://doi.org/10.15407/ujpe71.2.100.

[1] This work is based on the results presented at the 2025 "New Trends in High-Energy Physics" Conference.

arriving from all azimuthal angles φ_k and equipped with corresponding phase factors. We stress again that this delicate superposition is topologically protected by the phase vortex.

Extra care must be taken when dealing with vortex states of electrons, photons, and other particles with non-zero spin. Due to the intrinsic spin-orbit interaction that exists even in freely propagating fields [1], spin and OAM z-projections are, strictly speaking, not conserved separately. Still, exact monochromatic solutions of Maxwell's or Dirac's equations that describe vortex photons and electrons with definite longitudinal momentum k_z, modulus of the transverse momentum $\varkappa$, the total angular momentum j_z, and helicity λ have been constructed [6–9]. In addition, when $\tan\theta_k \equiv \varkappa/k_z \ll 1$, the paraxial approximation applies, and one can talk about approximately conserved spin and OAM.

Bringing together spin and OAM opens up an opportunity that is entirely impossible for plane waves. Namely, one can prepare a spin-OAM entangled state, which is characterized by a polarization *field* (spatially varying polarization vector) rather than a global polarization vector (see illustrations in Fig. 2). Potentially, this state will allow one to probe spin correlations at different points inside a composite system such as a nucleus or a hadron. There exist several schemes for preparing an initial state in such spin-OAM entangled states, including the very recent proposal [11] of transforming an initially non-vortex electron beam into such a state through its interaction with copropagating velocity-matched THz waveguide modes.

Let us also briefly overview the current experimental situation in the field. Vortex photons have been known and routinely used for decades. First produced for optical-range photons [12], they were recently demonstrated in the soft X-ray range in controllable single-OAM modes [13]. Very recently, evidence of production of vortex photons with $\ell = 7$ and energies up to 0.8 MeV was found in an all-optical tabletop experiment [14]. Numerous other proposals exist for producing high-energy photons either by direct emission in undulators and wigglers or via backscattering of low-energy photons from high-energy electrons [6] or relativistic ions [15], see more information in the review [4].

Ideas for the production of vortex electrons were put forth in [16], which led to their successful demonstration by several research groups [17–19]. At present, vortex electrons are usually produced in electron microscopes with moderately relativistic energies, $E_K = 300$ keV, but with extremely tight focusing down to the single-angstrom level. Impressive control over the OAM state, both in single mode and specific superpositions, has also been achieved [1]. Several proposals exist for bringing vortex electrons into multi-MeV or even GeV energies; they make use of electron emission inside magnetic fields [20], energy up-conversion via scattering [21], and the production of particles in heavy-ion collisions [22]. There is also ongoing theoretical and experimental work on the direct acceleration of lower energy vortex electrons inside a linac without disrupting their OAM properties [23–25].

Vortex states of cold neutrons [26, 27] and slow atoms [28] have also been demonstrated. In both cases, one first prepares a non-vortex wave packet of sufficiently large transverse coherence length, of the order of a micrometer, and then lets it pass through a fork diffraction grating that endows the wave packet with a non-zero OAM. Whether a similar approach will work for other hadrons, in particu-

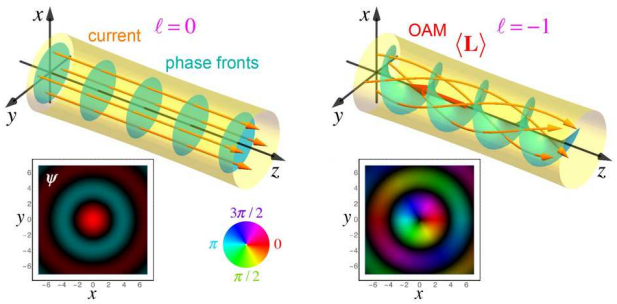

Fig. 1. The current lines and phase fronts of non-vortex Gaussian state (left) and an $\ell = -1$ vortex state (right). The insets show the intensity distributions in the transverse plane as well as the phase encoded in color. Adapted from [1]

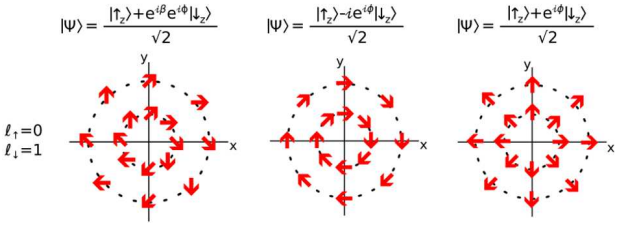

Fig. 2. Several examples of the spin-OAM entangled states of a spin-1/2 particle in vortex state that are described by polarization field rather than polarization vector. Adapted from [10]

lar, protons, antiprotons, and ions, requires dedicated experimental efforts. In particular, experimental vortex ion physics is included in the scientific program of the China Advanced Nuclear Physics Research Facility in Huizhou, China, which will enter operation in the near future [29].

To summarize, vortex states offer several key novelties that are unavailable in experiments with plane waves or broad Gaussian wave packets:

• a new adjustable degree of freedom, OAM, of the initial state;

• a very particular superposition of plane waves, which is topologically protected during wave packet propagation;

• exotic polarization opportunities offered by spin-OAM entangled states.

It is intriguing to explore what new insights into the structure and interactions of nuclei and hadrons will follow once collisions of MeV to GeV range vortex states become available.

2. Nuclear Physics Opportunities

One can benefit from the unique properties of vortex states already in single-vortex experiments, where a vortex photon, electron, or neutron is scattered or absorbed by a fixed microscopic target, such as an atom or a nucleus. An interesting proposal for making use of vortex electrons in nuclear physics was put forth in [30]. It is well known that nuclei of certain isotopes can exist in long-lived isomeric states, storing excitation energy for a long time. If one manages to control the evolution of the isomeric state, it would be possible to dramatically speed up its energy release. Various proposals have been discussed on how to trigger the transition of an isomer to a higher-lying gateway state followed by its prompt decay to the ground state, including the idea of using nuclear excitation by electron capture (NEEC) described in [31]. In the NEEC process, an external electron is captured on a vacant energy level of an atom or ion, but instead of emitting a photon, the energy is reabsorbed by the nucleus within the same atom or ion. The first experimental evidence of the ^{93m}Mo isomer depletion by the NEEC process was reported in 2018 [32], which immediately stirred some controversy [33].

This hot topic prompted the authors of [30] to suggest using vortex electrons for the NEEC process. Indeed, if the electron is to be captured onto an electronic orbital with a specific non-zero OAM, vortex electrons carrying an intrinsic OAM and a tailored wave function are ideally suited for this process. The authors of [30] predict an enhancement of up to four orders of magnitude in the depletion rate for the same isomer ^{93m}Mo compared to its spontaneous nuclear decay.

Another tantalizing opportunity for photonuclear processes was recently described in [34, 35]. It is well-known that the cross section of gamma photon absorption by a nucleus as a function of the photon energy displays a sequence of giant resonances in the MeV range. The dominant peaks are due to giant dipole resonances (GDR); higher multipole transitions are also possible but detecting them is extremely challenging due to the huge GDR background. However, a vortex photon carries a total angular momentum m_γ, which differs from helicity and can be adjusted externally. As a result, its absorption dramatically modifies the selection rules: if the nucleus is positioned exactly on the axis, transitions with multipolarity $J < m_\gamma$ are forbidden. By using vortex photons with $m_\gamma = 2$, one can fully suppress GDR and detect the otherwise weak giant quadrupole resonance. However, to realize this scheme, one must achieve subpicometer-scale precision for the location of the nucleus with respect to the vortex photon axis. If this challenge is met, one could achieve unprecedented control over nuclear transitions by selectively switching on and off specific multipolarities.

Vortex neutrons, too, can lead to novel nuclear effects. Consider, for example, the scattering of slow neutrons on a nucleus. As first realized by Schwinger in 1948 [36], the amplitude of this process contains not only the isotropic strong interaction contribution a but also the spin-dependent electromagnetic contribution that arises from the coupling between the neutron's magnetic moment and the electric field of the nucleus, which generates a non-zero magnetic field in the frame of the moving neutron. The total scattering amplitude for a plane-wave neutron is then

$$f_{\lambda\lambda'}(\mathbf{n},\mathbf{n}') = w'^{\dagger}_{\lambda'}(a + i\boldsymbol{\sigma}\cdot\mathbf{B})w_\lambda,$$
$$\mathbf{B} \propto \frac{[\mathbf{n}\times\mathbf{n}']}{(\mathbf{n}-\mathbf{n}')^2}, \tag{2}$$

where $\mathbf{n}$, $\mathbf{n}'$ are the unit vectors in the directions of the initial and final neutron, while w_λ and $w'_{\lambda'}$ are the corresponding spinors with helicities λ and λ'. If the incident neutron is polarized along the direction

$\boldsymbol{\zeta}$, the cross section summed over the final polarizations is

$$\frac{d\sigma(\mathbf{n},\mathbf{n}',\boldsymbol{\zeta})}{d\Omega'} = |a|^2 + |\mathbf{B}|^2 + 2(\mathbf{B}\cdot\boldsymbol{\zeta})\,\Im\, a. \tag{3}$$

One sees that this cross section is insensitive neither to the spin component ζ_z nor to the real part of the strong scattering amplitude.

These conclusions change if the incident neutron is in a vortex state [37, 38]. If a wave packet moves, on average, along the direction $\mathbf{n}$, it contains plane-wave components with various momenta $\mathbf{p}$, which are not parallel to $\mathbf{n}$ (see Fig. 3). The cross section is now peaked not in the forward direction but along the cone of directions defined by the plane-wave components $\mathbf{p}$. Moreover, due to the mismatch between $\mathbf{p}$ and $\mathbf{n}$, the cross section acquires sensitivity to both ζ_z and to $\Re\, a$. It is especially interesting that these effects are present even for very slow neutrons and can be tested at existing neutron facilities, provided that a sufficiently high flux of vortex neutrons is achieved.

We note in passing that the decay of the vortex neutron, or of the vortex muon, is of interest on its own right as it displays novel spectral-angular features that are further modified for spin-OAM entangled states [39–41].

3. Collisions of Vortex States: the Key Features

In particle and nuclear physics, the intrinsic OAM of the initial state represents a new, previously unexplored degree of freedom. It is interesting to understand what insights collisions of such states can offer [4]. One particularly intriguing opportunity would be to set up vortex electron-proton scattering, either elastic, inelastic, or deep inelastic, and gain new insights into the proton spin decomposition puzzle [42]. To clearly understand these new opportunities, one must begin by developing an appropriate description of collisions between two vortex states.

The theoretical investigation of high-energy collisions of vortex states began more than a decade ago [6, 7, 43, 44]. The key point is to realize that, when dealing with specific wave packets, one does not need to update the quantization procedure or generate a new set of Feynman rules; instead, plane-wave expressions can be reused by weighting them with appropriate momentum-space wave packets. The calculations are based on the formalism of general wave

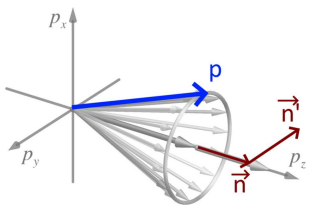

Fig. 3. Momentum space illustration of the vortex neutron: the cone represents the plane-wave components with momenta $\mathbf{p}$, which are not parallel to the average propagation direction $\mathbf{n}$. The scattered neutron moves alone $\mathbf{n}'$

packet scattering first developed in [45] and recently improved in [46]. Consider for definiteness a generic $2 \to 2$ scattering of plane waves with four-momenta k_1, k_2 into final-state plane waves with momenta k_1' and k_2'; we also denote the total final momentum by $K \equiv k_1' + k_2'$. The plane-wave S-matrix element is usually expressed as

$$S_{PW} = i(2\pi)^4\delta^{(4)}(k_1 + k_2 - K)\frac{\mathcal{M}}{\sqrt{16E_1E_2E_1'E_2'}}, \tag{4}$$

where $\mathcal{M} = \mathcal{M}(k_1, k_2; k_1', k_2')$ is calculated according to the standard Feynman rules. For non-plane-wave initial states, one introduces a suitably normalized momentum space wave function $\phi_i(k_i)$ and writes the S-matrix element as

$$S = \int \frac{d^3k_1}{(2\pi)^3}\frac{d^3k_2}{(2\pi)^3}\phi_1(k_1)\phi_2(k_2)S_{PW}. \tag{5}$$

The number of events per unit time is written as

$$d\nu = \frac{(2\pi)^7\delta(E)}{4E_1E_2}\,|f|^2\,\frac{d^3k_1'}{(2\pi)^3 2E_1'}\frac{d^3k_2'}{(2\pi)^3 2E_2'}\,, \tag{6}$$

where $\delta(E)$ stands for $\delta(E_1 + E_2 - E_1' - E_2')$ and the wave-packet-weighted amplitude is

$$f = \int \frac{d^3k_1}{(2\pi)^3}\frac{d^3k_2}{(2\pi)^3}\,\phi_1(k_1)\,\phi_2(k_2)\delta^{(3)}(\mathbf{k}_1 + \mathbf{k}_2 - \mathbf{K})\,\mathcal{M}. \tag{7}$$

The cross section is defined via $d\nu = d\sigma\cdot L$, with L being the luminosity function for the initial state wave packets. Its general expression in terms of Wigner's functions was derived in [46]; within the paraxial approximation, it can be simplified to

$$L = v_{\rm rel}\int d^3r\,dt\,|\psi_1(\mathbf{r},t)|^2|\psi_2(\mathbf{r},t)|^2, \tag{8}$$

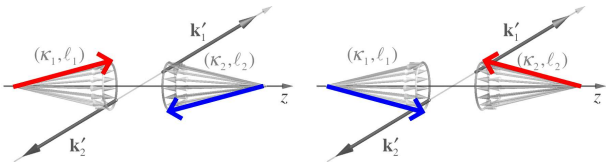

Fig. 4. Two pairs of plane-wave components in Bessel state collisions that lead to the same final state

where $v_{\rm rel}$ is the relative velocity between the centers of mass of the colliding wave packets.

A key novelty of vortex state collisions is a new dimension that appears in the final phase space distribution. Recall that, for plane-wave scattering, the transverse momentum differential cross section has the form

$$d\sigma_{\rm PW} \propto \delta^{(2)}(k_\perp)\,|\mathcal{M}|^2 d^2k'_{1\perp} d^2k'_{2\perp} = |\mathcal{M}|^2 d^2k'_{1\perp},$$

where $\delta^{(2)}(k_\perp)$ stands for $\delta^{(2)}(\mathbf{k}_{1\perp}+\mathbf{k}_{2\perp}-\mathbf{k}'_{1\perp}-\mathbf{k}'_{2\perp})$. Put simply, since the initial total momentum is fixed, the final total momentum $\mathbf{K}_\perp$ is also fixed. Therefore, for any value of the first final particle's momentum $\mathbf{k}'_{1\perp}$, the momentum of the second particle is uniquely defined. However, in vortex particle scattering, this intuition does not apply. The momentum delta function that enters the scattering amplitude f in Eq. (7) is smoothed out by the momentum space integration and disappears form the final phase space in Eq. (6). Thus, in the scattering of two vortex states, one can study distributions in $\mathbf{k}'_1$ and, simultaneously, in $\mathbf{k}'_2$. Alternatively, one can explore a distribution in the total transverse momentum $\mathbf{K}_\perp$, a feature that was altogether impossible in plane-wave collisions. It is this new dimension in the final state phase space that exhibits various interference effects that can be used to probe the scattering process in a novel way.

4. Novel Opportunities in Vortex State Scattering

Consider, for definiteness, the collision of two Bessel vortex states. It follows from Eq. (1) and momentum conservation that, for each kinematically available total transverse momentum from the annular region $|\varkappa_1 - \varkappa_2| \leq K_\perp \leq \varkappa_1 + \varkappa_2$, one can find exactly two initial-state plane-wave pairs contained within the corresponding Bessel states that lead to the same final state with $\mathbf{k}'_1$ and $\mathbf{k}'_2$, as schematically shown in Fig. 4. The plane-wave scattering amplitudes corresponding to different initial states yet leading to the same final state interfere [44, 47–49]:

$$\begin{aligned} f &= c_a\,\mathcal{M}_a(k_{1a}, k_{2a}; k'_1, k'_2) + \\ &+ c_b\,\mathcal{M}_b(k_{1b}, k_{2b}; k'_1, k'_2), \\ d\sigma &\propto |c_a\mathcal{M}_a + c_b\mathcal{M}_b|^2. \end{aligned} \tag{9}$$

As a result, one expects interference fringes in the annular region of $\mathbf{K}_\perp$, which depend on the magnitude of $|\mathbf{K}_\perp|$ via the oscillatory coefficients c_a and c_b (see Fig. 5).

Even more remarkable is that this interference pattern allows access to the scattering angle-dependent phase of the overall scattering amplitude. Consider elastic electron-electron scattering. At tree level, the scattering amplitude is real with a suitable choice of spinors, but multi-photon exchanges generate an additional phase factor that depends on the scattering angle. Consequently, the total plane-wave scattering amplitude can be written schematically as

$$\mathcal{M} = |\mathcal{M}|e^{i\Phi(\theta)}, \quad \Phi(\theta) \approx \Phi_0 + 2\alpha_{em}\ln(1/\theta). \tag{10}$$

The so-called Coulomb phase $\Phi(\theta)$ depends on the scattering angle and its exact definition has been a matter of debate since the 1960s. In plane-wave scattering, the differential cross section is $d\sigma \propto |\mathcal{M}|^2$, which is insensitive to the phase. The same issue of an unknown overall phase arises in hadron scattering, such as high-energy pp or $p\bar{p}$ scattering, as well as the low-energy photoproduction of strange hadrons, such as $\gamma p \to K^+\Lambda$. Such processes are notorious due to the many interfering partial waves, and it has been repeatedly stated that the analysis would benefit significantly if we could measure the overall phase of the amplitude [50].

It turns out that vortex scattering indeed offers access to the θ-behavior of the total scattering amplitude. The two interfering amplitudes in Eq. (9), $\mathcal{M}_a$ and $\mathcal{M}_b$, correspond to two different scattering angles θ_a and θ_b. Therefore, they have a relative phase, which leads to a peculiar distortion of the interference pattern visible in Fig. 5, right, and can be extracted from experimental data through a suitable asymmetry [48].

A similar analysis was recently presented for the vortex $p\bar{p} \to e^+e^-$ annihilation [51]. Here, one must consider the electromagnetic form factors of the proton G_E and G_M in the timelike region, where they acquire phases, and the possible relative phase between

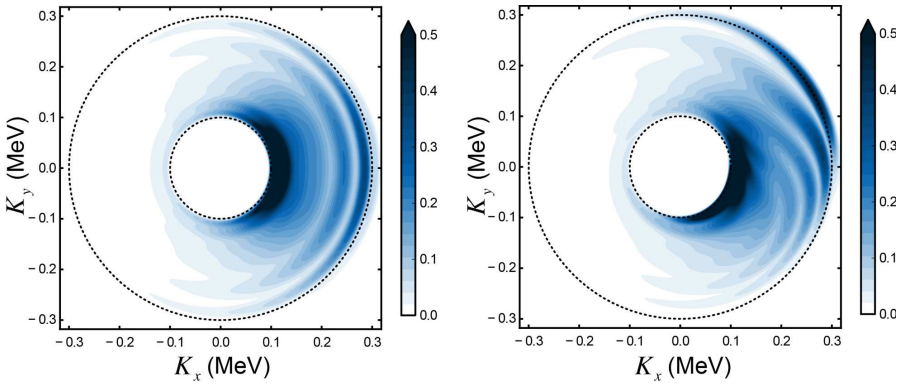

Fig. 5. Interference fringes in the $\mathbf{K}_\perp$ distribution in elastic scattering of two Bessel-state electrons. The Coulomb scattering amplitude is either purely real (left) or bears an additional phase factor with an artificially enhanced Coulomb phase (right). Adapted from [48]

them can be extracted from a similar distortion of the interference fringes. Furthermore, the technique for extracting additional features of the scattering amplitude unavailable in plane-wave collisions can be generalized to other forms of waveform-engineered wave packets [5].

Another impressive, and even counterintuitive, feature of vortex state collisions is that they allow one to study spin-dependent quantities in a fully inclusive and unpolarized setting [52, 53]. Let us illustrate this with the example of a generic vector meson production in vortex e^+e^- annihilation.

We begin with a plane-wave collision and use a simple Ansatz for the transition amplitude:

$$\mathcal{M}_{\zeta_1\zeta_2\lambda_V} = g\,\bar{v}_{\zeta_2}(k_2)\,\gamma_\mu\,u_{\zeta_1}(k_1)\,V^{\mu *}_{\lambda_V}(K) \propto$$
$$\propto \lambda_V \cos\theta_V + 2\zeta. \qquad (11)$$

Here, $\zeta \equiv \zeta_1 = -\zeta_2 = \pm 1/2$ and $\lambda_V = -1, 0, +1$ are the helicities of e^-, e^+, and the vector meson V, respectively. The amplitude depends on the helicities, and so does the differential cross section:

$$d\sigma_{\rm PW} \propto 1 + \cos^2\theta_V + 2\lambda_V \cdot (2\zeta) \cdot \cos\theta_V. \qquad (12)$$

However, if the initial e^+e^- pair is unpolarized, the last term drops, and the produced meson is unpolarized as well: $d\sigma_{\rm PW}(\lambda_V = +1) = d\sigma_{\rm PW}(\lambda_V = -1)$.

The above result may seem totally obvious. However, this intuition fails for vortex e^+e^- annihilation. As discussed above, the momentum of the final vector meson $\mathbf{K}$ is not fixed, so that one can study differential distribution in the transverse plane $\mathbf{K}_\perp$. Computation of the amplitude presented in [52, 53] can be schematically written as

$$\mathcal{M}_{\zeta,-\zeta,\lambda_V} \propto (\lambda_V \cos\theta_V + 2\zeta) \cdot (c_1 + 2\zeta \cdot c_2), \qquad (13)$$

where c_1 and c_2 are the oscillating factors that depend on $K_\perp$, just as in Eq. (9). As a result, the cross section for the unpolarized vortex e^+e^- annihilation reads:

$$d\sigma_{\rm v} \propto (c_1^2 + c_2^2)(1 + \cos^2\theta_V) + 2c_1c_2\lambda_V \cos\theta_V. \qquad (14)$$

We arrive at a remarkable conclusion: the vector meson ejected at specific polar angle θ_V is partially polarized, even though it is produce in unpolarized vortex electron and positron collision.

The explanation of this puzzling effect comes from the intrinsic spin-orbit interactions within the free-propagating fermions. When we define an unpolarized *vortex* electron, we assume that it carries a well-defined (half-integer) total angular momentum j. This electron wave can be found in the helicity states with $\zeta = +1/2$ or $-1/2$ with equal probabilities. However, due to the spin-orbit interaction, these two helicity components exhibit different spatial arrangements. Therefore, when two such states collide, the collision probabilities for the two helicity options can be distinct and production-angle dependent. This non-equivalent spatial organization serves as a bias towards one or the other sign λ_V.

We conclude by noting that it is precisely this new way to access spin-dependent properties of the proton, or other hadrons, that makes vortex state collisions a potentially intriguing tool for understanding the proton spin structure [42]. One can envision the vortex version of deep-inelastic scattering (DIS), in which both the electron and the proton are in the vortex state. By making use of the new kinematical dimension and novel observables and structure functions, one can probe the transverse-momentum dependent spin structure of the proton in a more inclusive, less differential way. Although the potential

application of vortex scattering to the proton spin structure was already mentioned in the first paper on vortex-vortex scattering [44], no dedicated study of vortex DIS has been published so far. This represents one of the most promising directions for future theoretical work in the physics of vortex states.

5. Conclusions

In summary, the physics of vortex states is an emerging interdisciplinary field that links beam physics, atomic physics, optics, nuclear, and particle physics. Vortex states offer new degrees of freedom never before used in nuclear and particle physics: adjustable, topologically protected initial-state OAM, new dimensions in the final phase space, and spin-OAM entanglement, which provide much richer polarization options. Remarkable effects, hard or impossible to observe with plane-wave scattering, are theoretically predicted and await experimental verification. While experimental progress is slow due to significant challenges, recent results inspire hope that within a decade we will have access to multi-MeV vortex electrons, photons, or hadrons. It is timely to gather further theoretical input on the novel opportunities offered by vortex states across various branches of physics.

The author expresses sincere gratitude to the conference organizing team from Taras Shevchenko National University of Kyiv and the local organizers from Batumi Shota Rustaveli State University for their dedication and hard work, which was particularly challenging in the wake of the tragic loss of Prof. László Jenkovszky, the long-time leader of the conference series.

1. K.Y. Bliokh, I.P. Ivanov, G. Guzzinati, L. Clark, R. Van Boxem, A. Béché, R. Juchtmans, M.A. Alonso, P. Schattschneider, F. Nori *et al.* Theory and applications of free-electron vortex states. *Phys. Rept.* **690**, 1-70 (2017).
2. S.M. Lloyd, M. Babiker, G. Thirunavukkarasu, J. Yuan. Electron vortices: Beams with orbital angular momentum. *Rev. Mod. Phys.* **89**, 035004 (2017).
3. B.A. Knyazev, V.G. Serbo. Beams of photons with nonzero projections of orbital angular momenta: new results. *Phys. Uspekhi* **61**, 449 (2018).
4. I.P. Ivanov. Promises and challenges of high-energy vortex states collisions. *Prog. Part. Nucl. Phys.* **127**, 103987 (2022).
5. D. Karlovets. Scattering of wave packets with phases. *JHEP* **03**, 049 (2017).
6. U.D. Jentschura, V.G. Serbo. Generation of high-energy photons with large orbital angular momentum by compton backscattering. *Phys. Rev. Lett.* **106** (1), 013001 (2011).
7. D.V. Karlovets Electron with orbital angular momentum in a strong laser wave. *Phys. Rev. A* **86**, 062102 (2012).
8. K.Y. Bliokh, M.R. Dennis, F. Nori. Relativistic electron vortex beams: Angular momentum and spin-orbit interaction. *Phys. Rev. Lett.* **107**, 174802 (2011).
9. V. Serbo, I.P. Ivanov, S. Fritzsche, D. Seipt, A. Surzhykov. Scattering of twisted relativistic electrons by atoms. *Phys. Rev. A* **92** (1), 012705 (2015).
10. D. Sarenac, J. Nsofini, I. Hincks, M. Arif, Ch. W. Clark, D.G. Cory, M.G. Huber, D.A. Pushin. Methods for preparation and detection of neutron spin-orbit states. *New J. Phys.* **20** 103012 (2018).
11. Z.P. Li, Y. Wang, Y.I. Salamin, M. Ababekri, F. Wan, Q. Zhao, K. Xue, Y. Tian, J.X. Li. Generation of relativistic structured spin-polarized lepton beams. *Phys. Rev. Lett.* **135** (13), 135001 (2025).
12. L. Allen, M.W. Beijersbergen, R.J.C. Spreeuw, J.P. Woerdman. Orbital angular momentum of light and the transformation of Laguerre–Gaussian laser modes. *Phys. Rev. A* **45**, 8185 (1992).
13. J.C.T. Lee, S.J. Alexander, S.D. Kevan, S. Roy, B.J. McMorran. Laguerre–Gauss and Hermite–Gauss soft X-ray states generated using diffractive optics. *Nature Photonics* **13**, 205 (2019).
14. M. Wei, S. Chen, Y. Wang, X. Hu, M. Zhu, H. Hu, P. L. He, W. Zhou, J. Jia, L. Lu *et al.* Experimental evidence of vortex *Oi* photons in all-optical inverse compton scattering. arXiv:2503.18843 [physics.plasm-ph].
15. V.G. Serbo, A. Surzhykov, A. Volotka. Resonant scattering of plane-wave and twisted photons at the gamma factory. *Annalen Phys.* **534** (3), 2100199 (2022).
16. K.Y. Bliokh, Y.P. Bliokh, S. Savel'ev, F. Nori, Semiclassical dynamics of electron wave packet states with phase vortices. *Phys. Rev. Lett.* **99**, 190404 (2007).
17. M. Uchida, A. Tonomura. Generation of electron beams carrying orbital angular momentum. *Nature* **464**, 737 (2010).
18. J. Verbeeck, H. Tian, P. Schlattschneider. Production and application of electron vortex beams. *Nature* **467**, 301 (2010).
19. B.J. McMorran *et al.* Electron vortex beams with high quanta of orbital angular momentum. *Science* **331**, 192 (2011).
20. D. Karlovets. Vortex particles in axially symmetric fields and applications of the quantum Busch theorem. *New J. Phys.* **23** (3), 033048 (2021).
21. D.V. Karlovets, S.S. Baturin, G. Geloni, G.K. Sizykh, V.G. Serbo. Shifting physics of vortex particles to higher energies via quantum entanglement. *Eur. Phys. J. C* **83** (5), 372 (2023).
22. L. Zou, P. Zhang, A.J. Silenko. Production of twisted particles in heavy-ion collisions. *J. Phys. G* **50** (1), 015003 (2023).
23. S.S. Baturin, D.V. Grosman, G.K. Sizykh, D.V. Karlovets. Evolution of an accelerated charged vortex particle in

an inhomogeneous magnetic lens. *Phys. Rev. A* **106** (4), 042211 (2022).
24. D. Karlovets, D. Grosman, I. Pavlov. Angular momentum dynamics of vortex particles in accelerators. arXiv: 2507.08763 [physics.acc-ph].
25. A.S. Dyatlov et al. Classical and Quantum Beam Dynamics Simulation of the RF Photoinjector Test Bench at JINR. arXiv:2509.00732 [physics.acc-ph].
26. Ch.W. Clark, R. Barankov, M.G. Huber, M. Arif, D.G. Cory, D.A. Pushin. Controlling neutron orbital angular momentum. *Nature* **525**, 504 (2015).
27. D. Sarenac *et al.* Experimental realization of neutron helical waves. *Sci. Adv.* **8**, eadd2002 (2022).
28. A. Luski *et al.* Vortex beams of atoms and molecules. *Science* **373** (6559), 1105 (2021).
29. F. An, D. Bai, S. Chen, X. Chen, H. Duyang, L. Gao, S.F. Ge, J. He, J. Huang, Z. Huang, *et al.* High-precision physics experiments at huizhou large-scale scientific facilities. arXiv:2504.21050 [hep-ph].
30. Y. Wu, S. Gargiulo, F. Carbone, C.H. Keitel, A. Pálffy. Dynamical control of nuclear isomer depletion via electron vortex beams. *Phys. Rev. Lett.* **128** (16), 162501 (2022).
31. A. Palffy, J. Evers, C.H. Keitel. Isomer triggering via nuclear excitation by electron capture. *Phys. Rev. Lett.* **99**, 172502 (2007).
32. C.J. Chiara *et al.* Isomer depletion as experimental evidence of nuclear excitation by electron capture. *Nature* **554** (7691), 216 (2018).
33. Y. Wu, C.H. Keitel, A. Pálffy. ^{93m}Mo isomer depletion via beam-based nuclear excitation by electron capture. *Phys. Rev. Lett.* **122** (21), 212501 (2019).
34. Z.W. Lu, L. Guo, Z.Z. Li, M. Ababekri, F.Q. Chen, C. Fu, C. Lv, R. Xu, X. Kong, Y.F. Niu *et al.* Manipulation of giant multipole resonances via vortex γ photons. Phys. *Rev. Lett.* **131** (20), 202502 (2023).
35. Z.W. Lu, H. Zhang, T. Li, M. Ababekri, X. Wang, J.X. Li. Nuclear excitation and control induced by intense vortex laser. arXiv:2503.12812 [nucl-th].
36. J. Schwinger. On the polarization of fast neutrons. *Phys. Rev.* **73**, 407 (1948).
37. A.V. Afanasev, D.V. Karlovets, V.G. Serbo. Schwinger scattering of twisted neutrons by nuclei. *Phys. Rev. C* **100** (5), 051601 (2019).
38. A.V. Afanasev, D.V. Karlovets, V.G. Serbo. Elastic scattering of twisted neutrons by nuclei. *Phys. Rev. C* **103** (5), 054612 (2021).
39. P. Zhao, I.P. Ivanov, P. Zhang. Decay of the vortex muon. *Phys. Rev. D* **104** (3), 036003 (2021).
40. W. Kou, B. Guo, X. Chen. Unveiling the secrets of vortex neutron decay. *Phys. Lett. B* **862**, 139332 (2025).
41. I. Pavlov, A. Chaikovskaia, D. Karlovets. Angular momentum effects in neutron decay. *Phys. Rev. C* **111** (2), 024619 (2025).
42. C.A. Aidala, S.D. Bass, D. Hasch, G.K. Mallot. The spin structure of the nucleon. *Rev. Mod. Phys.* **85**, 655 (2013).
43. U.D. Jentschura, V.G. Serbo. Compton upconversion of twisted photons: Backscattering of particles with nonplanar wave functions. *Eur. Phys. J. C* **71**, 1571 (2011).
44. I.P. Ivanov. Colliding particles carrying non-zero orbital angular momentum. *Phys. Rev. D* **83**, 093001 (2011).
45. G.L. Kotkin, V.G. Serbo, A. Schiller. Processes with large impact parameters at colliding beams. *Int. J. Mod. Phys. A* **7**, 4707 (1992).
46. D.V. Karlovets, V.G. Serbo. Effects of the transverse coherence length in relativistic collisions. *Phys. Rev. D* **101** (7), 076009 (2020).
47. I.P. Ivanov. Measuring the phase of the scattering amplitude with vortex beams. *Phys. Rev. D* **85**, 076001 (2012).
48. I.P. Ivanov, D. Seipt, A. Surzhykov, S. Fritzsche. Elastic scattering of vortex electrons provides direct access to the Coulomb phase. *Phys. Rev. D* **94** (7), 076001 (2016).
49. D.V. Karlovets. Probing phase of a scattering amplitude beyond the plane-wave approximation. *EPL* **116** (3), 31001 (2016).
50. Y. Wunderlich, R. Beck, L. Tiator. The complete-experiment problem of photoproduction of pseudoscalar mesons in a truncated partial-wave analysis. *Phys. Rev. C* **89** (5), 055203 (2014).
51. N. Korchagin. Studying timelike proton form factors using vortex state $p\bar{p}$ annihilation. *Phys. Rev. D* **111** (7), 076005 (2025).
52. I.P. Ivanov, N. Korchagin, A. Pimikov, P. Zhang. Doing spin physics with unpolarized particles. *Phys. Rev. Lett.* **124** (19), 192001 (2020).
53. I.P. Ivanov, N. Korchagin, A. Pimikov, P. Zhang. Twisted particle collisions: a new tool for spin physics. *Phys. Rev. D* **101** (9), 096010 (2020).

Received 05.11.20

І.П. Іванов

ВИХРОВІ СТАНИ ЯК НОВИЙ ІНСТРУМЕНТ ДЛЯ ЯДЕРНОЇ ФІЗИКИ ТА ФІЗИКИ ЧАСТИНОК

Вихрові стани фотонів, електронів та інших частинок – це хвильові пакети зі спіральними хвильовими фронтами, які несуть проекцію власного орбітального кутового моменту (ОКМ) вздовж свого середнього напрямку поширення. Такі стани вже були отримані експериментально, хоча й при низьких енергіях, і існують перспективи поширити їх на діапазони енергій порядку МеВ та ГеВ. Регульований ОКМ, що переноситься такими хвильовими пакетами, являє собою абсолютно новий ступінь вільності, який ніколи не використовували у зіткненнях частинок та ядер. Передбачаючи майбутній експериментальний прогрес, можна запитати, які знання про ядра та частинки можна отримати, коли зіткнення високоенергетичних вихрових станів стануть можливими. В даній роботі ми обговорюємо сучасну ситуацію та окреслюємо фізичні можливості, які пов'язані із зіткненнями високоенергетичних вихрових станів.

Ключові слова: вихрові стани, орбітальний кутовий момент, загадка протонного спіну.